



Monte Carlo Evaluation of Dose Enhancement Due to CuATSM or GNP Uptake in Hypoxic Environments with External Beam Radiation

This article was published in the following Dove Press journal:
International Journal of Nanomedicine

Stephen Martinez
Alexander Brandl 
Del Leary 

Department of Environmental and
Radiological Health Sciences, Colorado
State University, Fort Collins, CO, USA

Purpose: Most solid tumors contain areas of chronic hypoxia. Gold nanoparticles (GNP) have been extensively explored as enhancers of external beam radiation; however, GNP have lower cellular uptake in hypoxic conditions than under normoxic conditions. Conversely, the chelator diacetyl-bis (N(4)-methylthiosemicarbazonato) copper II (CuATSM) deposits copper in hypoxic regions, allowing for dose enhancement in previously inaccessible regions.

Methods: External beam sources with different spectra were modeled using a Monte Carlo code (EGSnrc) to evaluate radioenhancement in a layered model with metal solutions. Also considered was a simple concentric layered tumor model containing a hypoxic core with each layer varying in concentrations of either copper or gold according to hypoxic conditions. Low energy external photon beams were then projected onto the tumor to determine the regional dose enhancement dependent on hypoxic conditions.

Results: Dose enhancement was more pronounced for beam spectra with low energy photons (225 kVp) and was highly dependent on metal concentrations from 0.1 g/kg to 100 g/kg. Increasing the depth of the metallic solution layer from 1 cm to 6 cm decreased dose enhancement. A small increase in the dose enhancement factor (DEF) of 1.01 was predicted in the hypoxic regions of the tumor model with commonly used diagnostic concentrations of CuATSM. At threshold concentrations of toxic subcutaneous injection levels, the DEF increases to 1.02, and in simulation of a high concentration of CuATSM, the DEF increased to 1.07. High concentration treatments are also considered, as well as synergistic combinations of GNP/CuATSM treatments.

Conclusion: The research presented is novel utilization of CuATSM to target hypoxic regions and act as a radiosensitizer by the nature of its ability to deposit copper metal in reduced tissue. We demonstrate CuATSM at high concentrations with low energy photons can increase dose deposition in hypoxic tumor regions.

Keywords: radiosensitivity, modeling, hypoxia, radiation therapy

Introduction

Most solid tumors contain micro-regions under hypoxic conditions.¹ Although hypoxic conditions can be dynamic, often areas of chronic hypoxia, caused by limited diffusion of oxygen from tumor microvasculature exist within the central region.² In the treatment of cancer through radiation, these regions often have increased resistance to conventional radiotherapy.^{2,3} Hypoxic radioresistance is not entirely understood but may be caused in part by the lack of oxygen and other reactive oxygen species (ROS) acting to produce permanent DNA damage as a result of ionizing radiation.^{4,5} In order

Correspondence: Stephen Martinez
Email skmartin@colostate.edu

to overcome the radioresistance in hypoxic tumor areas, radiosensitizers have been considered to enhance radiation dose within these radioresistant regions.

Metal radiosensitizers are one class of hypoxic radiosensitizers that has been widely explored. Earlier investigations have established that high Z elements without chemical toxicity in low energy x-ray beams result in increased dose due to additional electrons emitted by the photoelectric interaction.^{6,7} Additionally, excited elements decay through atomic relaxation and emit Auger electrons, which in close proximity to DNA causes damage in a manner comparable with high linear energy transfer (LET) particles.^{6,8} In recent years, gold nanoparticles (GNP) have been explored for their potential in cancer therapy as an enhancer of external beam radiation because of their low toxicity, high photoelectric cross-section, and ability to be manipulated allowing hydrophilic coatings and attachment of antibodies which can increase cellular uptake.^{9–11} Numerous studies have demonstrated the efficacy of GNP to enhance dose.^{12–15} A limitation of nanoparticles is that they enter tumor cells peripherally located near “leaky” vessels and are limited in the distance they diffuse through tissue.^{11,16–18} Experiments conducted with GNP found a decrease in cellular uptake in anoxic and hypoxic conditions likely as a result of those cells having less energy with which to uptake external particles, although this may only be the case in acute hypoxic conditions.^{19,20}

⁶⁴CuATSM (diacetyl-bis N4-methylthiosemicarbazone) is used as positron emitting tomography (PET) agent; the ATSM ligand has been shown to deposit its metal ion (copper or zinc) preferentially in hypoxic tissues, although there are cell type specific differences.^{21–24} Bioreductive electron donating enzymes present in the microsomes or cytosol act to reduce Cu(II)ATSM to Cu(I)ATSM, the charged form has decreased permeability to cell membranes and enhanced retention in hypoxic conditions.^{21,25}

Hypoxia targeting intensity-modulated radiation therapy (IMRT) has been investigated using radioactive CuATSM as a method to identify hypoxic regions and overcome tumor radioresistance by improved targeting and dose escalation within a hypoxic region.^{26,27} Additionally, radiotheranostic treatment has been suggested utilizing ⁶⁴CuATSM that targets the hypoxic tumor tissue and enhances tumor killing by microscopic emission of Auger electrons in proximity to the DNA.^{22,28–31} A current challenge of using ⁶⁴CuATSM as a theranostic agent is that it has been shown to accumulate

in other low oxygen areas, such as in the intestines and liver.^{24,32}

This investigation analyzes the radiosensitizing potential of non-radioactive CuATSM in combination with external beam radiation using Monte Carlo numerical modeling. External beam spectra are modeled to irradiate water phantoms containing metal solution layers to evaluate dose enhancement parameters of concentration and depth. The phantom geometry is then altered to approximate a simple hypoxic tumor. Using tumor uptake values for GNP and CuATSM from literature, copper and gold concentration are determined for tumor regions and modeled to evaluate dose enhancement to hypoxic regions.

Materials and Methods

External radiation source models were created using EGSnrc, a Monte Carlo software toolkit for the passage of electrons and photons through matter.³³ All simulations were run on the Rocky Mountain Advanced Computing Consortium (RMAACC) Summit supercomputer running Red Hat Enterprise Linux Server 7.3 with access to up to 904 Intel Xeon E5-2680 v3 processors 12 cores X 2.5 GHz.³⁴ The BEAMnrc code, specializing in simulating radiation beams from radiotherapy units, was used to create three beam sources with differing photon spectra.³⁵ In each case, a phase space file of at least 10^9 particles was created with each particle's positional information upon exiting the beam source model. Several runs of 10^9 initial histories with different random number generator seeds were combined utilizing the addphsp utility to create the phase space, and spectral distributions were calculated using BEAMdp. In all cases, EGSnrc physics parameters were modified to allow for electron impact ionization, Rayleigh scattering, atomic relaxations, and photoelectric angular sampling to enhance low energy tracking. Beam sources were composed of International Commission on Radiation Units and Measurements (ICRU) materials edited with Pegs4 to have lower energy cutoffs of 512 keV (including rest mass energy) for electrons and 1 keV for photons.

An approximate model for the Varian Trilogy linear accelerator head was created using the High-Energy Clinac package available by non-disclosure agreement and benchmarked against clinical beam data for 6 MV photons. Variance reduction included directional bremsstrahlung splitting with splitting number 29 and a splitting field radius of 10 cm at a source to surface distance (SSD) of 100 cm. Energy cutoffs for photons (PCUT) and electrons (ECUT)

were set to 1 keV and 20 keV, respectively, with higher cutoff values (ECUTIN) for electrons within the primary collimator, the flattening filter, the jaws, and the MLC based on the electron range in those materials. A lower-energy flattening filter-free (FFF) linac with maximum energy 2.35 MV was created by altering the Clinac design with a low-Z target composed of graphite and removal of the flattening filter.^{12,36} Uniform bremsstrahlung splitting with splitting number 29 was used with the same ECUT and PCUT as before. Finally, a low energy beam (225 kVp) was created to model the small animal radiotherapy research platform (SARRP) from schematics and models provided by Xstrahl Medical Systems for a 5 mm x 5 mm nozzle.³⁷ Uniform bremsstrahlung splitting with splitting number 300 was used in this case with electron range rejection of 10 MeV. Normalized photon spectra and percentage depth dose for these external beam sources are shown in Figure 1.

Layered Phantom Model with Metal Solution

Dose in voxel phantoms was analyzed using the DOSXYZnrc package. Composite phase space files were used as sources incident on the phantom with 100 cm SSD for the linac cases and 34 cm SSD for the SARRP. The phantom was a rectangular prism with dimensions (and voxel dimensions) 30 cm (0.5 cm) x 30 cm (0.5 cm) x 8 cm (0.05 cm) in the x, y, and z dimensions, respectively. Pure water was used as the base material with

inhomogeneities introduced as slabs perpendicular to the beam at varying depths within the phantom (Figure 2).

$$DEF = \frac{D_{metal\ solution}}{D_{water}} \quad (1)$$

Twenty-five 0.5 cm voxels over 2.5 cm in x and y are averaged to improve the signal-to-noise ratio. Within the water phantom, a 1 cm layer of metal solution with concentrations of 100 mg/g for both gold and copper (Figure 2A) is placed at a depth of 3 cm. The dose is then calculated within this phantom to determine the dose enhancement factor (DEF) of each beam energy.

$$Concentration = \frac{M_{metal}}{M_{metal+water}} \quad (2)$$

The composition and densities of the inhomogeneities' materials were altered from pure water using Peps4 to contain varying concentrations of copper or gold ranging from 0.1 g/kg to 100 g/kg to be analyzed for their dose enhancing potential. The depths of the inhomogeneities were varied to analyze the effects of beam hardening (Figure 2B).

Hypoxic Tumor Model

Simple geometrical representations have previously served as tumor models, as they provide a basis for extension to more complex features.^{2,12,38-40} A cuboidal phantom with dimensions 5 cm x 5 cm x 5 cm with pure water as base material was used to simulate a simple 125 mm³ tumor with a 8 mm³ hypoxic core with differential uptakes of metal by oxygen

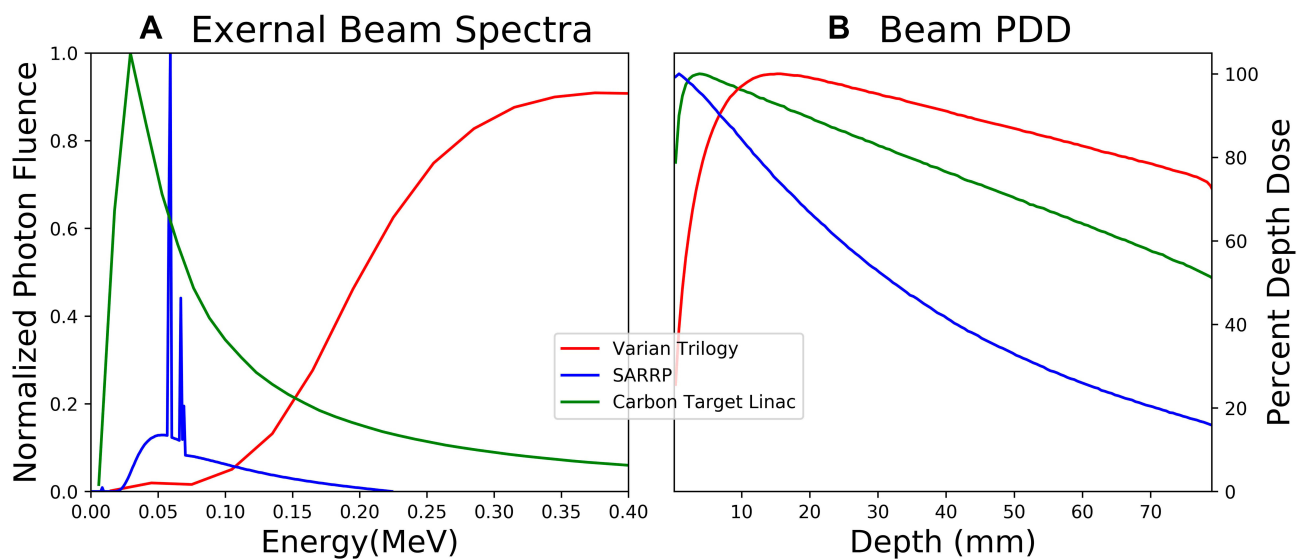


Figure 1 (A) Beam spectra evaluated for the evaluated external radiation sources. Photon fluence is normalized to maximum. (B) Percentage depth dose (PDD) for same beam spectra in water phantom.

Abbreviation: SARRP, Small Animal Radiation Research Platform.

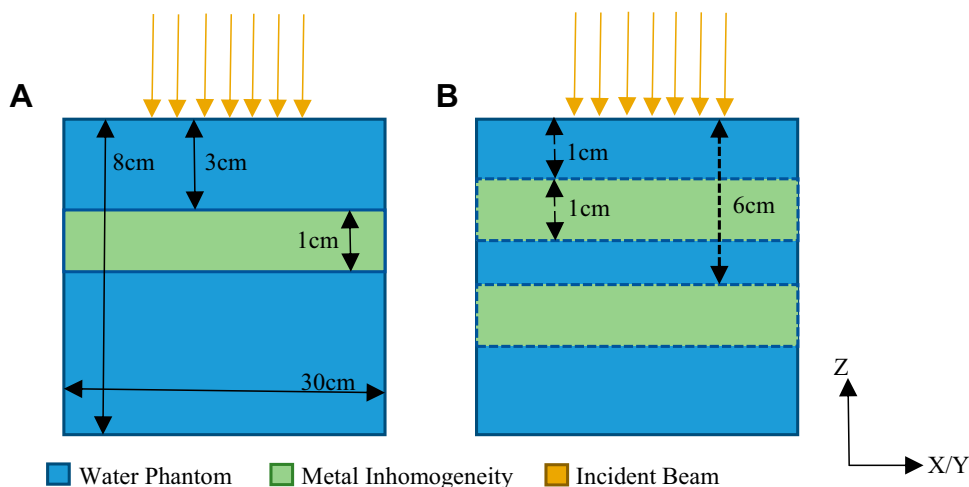


Figure 2 Geometries for simulation of dose in voxelized phantom, not to scale (A) 1 cm multi-layer phantom with metal solution layer extending the dimensions of the phantom in X/Y (B) 1 cm metal solution layer depth changed from top at 1 cm to 6 cm changed in 1 cm steps.

concentration (Figure 3).^{19,21,41,42} The DEF in the hypoxic tumor model was calculated for the low energy SARRP beam as it resulted in the most enhancement in the phantom model. In all cases, normal tissue, surrounding the simulated tumor was assumed to have zero uptake of radiosensitizing metal.^{38–40} Within the tumor, uptake of gold or copper was determined for normoxic and hypoxic tissue uptake.

Gold Nanoparticle Tumor Concentrations

For GNP simulations, concentrations were informed by a previous mouse study where 1.35 g/kg (GNP/bodyweight) was injected intravenously and deposited from the circulation into the tumor.⁴³ In vitro, it was found that GNP uptake into

cells was decreased by a factor of approximately 3.4 in anoxic compared to normoxic conditions.¹⁹ In addition, the degree of GNP uptake decreases in volumetric tumors distant from the vasculature due to the low diffusion of GNP in tissue.^{17,18,39} Under these assumptions, the DEF was calculated for a concentration of 1.35 g/kg assuming direct injection into the tumor. Uptake for GNP in the hypoxic region was then evaluated at a decreased concentration (Reduced) for decreased uptake due to anoxic conditions alone, and zero concentration of GNP uptake (Zero) for considerations of cell layer blocking diffusion (Table 1).

CuATSM Tumor Concentrations

Previous studies using mice with induced tumors found that ⁶⁴Cu-ATSM has a high deposition in over-reduced hypoxic regions of tumor tissue.⁴² Additionally, cell models have indicated that uptake of CuATSM is about 9 times greater in anoxic regions than in normoxic conditions for certain cell lines.⁴¹ The radioactive isotope ⁶⁴Cu has a half-life 12.7 hours and decays by 17.86 (± 0.14)% by positron emission to ⁶⁴Ni, 39.0 (± 0.3)% by beta decay to ⁶⁴Zn, 43.075 (± 0.500)% by electron capture to ⁶⁴Ni, and 0.475 (± 0.010)% gamma radiation/internal conversion. The position component allows for PET imaging and the beta decay creates additional local dose deposition and allows for theranostic applications. Studies using non-radioactive CuATSM systemic injections for treatment of motor neuron disease have limited concentration levels at approximately 0.1 g/kg due to the concerns of the toxicity of the CuATSM solvent dimethyl sulfoxide (DMSO).^{44,45} Copper was assumed to comprise 19.7% by mass of the CuATSM chelate in these simulations.⁴⁷

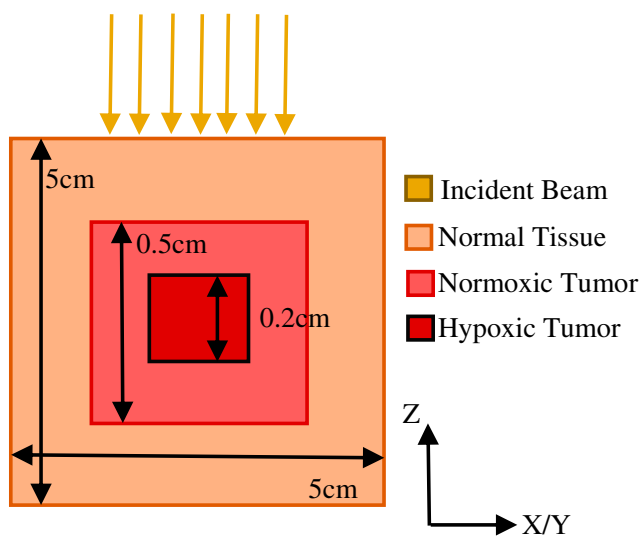


Figure 3 Tumor model geometry with phantom representing a tumor with normoxic and hypoxic regions.

Table 1 Summary of Metal Concentrations Evaluated for Dose Enhancement in Hypoxic Tumor

| Material | | Injection Concentration [g/kg] | Metal Concentration Normoxic [g/kg] (Factor) | Metal Concentration Anoxic [g/kg] (Factor) |
|----------|----------------------------|--------------------------------|--|--|
| GNP | Reduced Zero | 1.35 | 1.35 (1) | 0.397 (1/3.4) |
| | | 1.35 | 1.35 (1) | 0 (0) |
| CuATSM | Low | 0.1 | 0.0197 (0.197) | 0.177 (9) |
| | Medium | 0.34 | 0.0672 (0.197) | 0.605 (9) |
| | High (Theoretical) | 1.35 | 0.27 (0.197) | 2.39 (9) |
| | Very High (Theoretical) | 6.85 | 1.35 (0.197) | 12.1 (9) |
| Hybrid | Mix (Theoretical) | 1.35 (GNP) | 1.35 (GNP) | 4.68 (CuATSM) |
| | | 2.6 (CuATSM) | | |

Abbreviations: GNP, gold nanoparticle; CuATSM, Cu(II) diacetyl-bis N4-methylthiosemicarbazone.

Therefore, assuming a direct tumor injection, having the highest potential concentrations, at (0.1 g/kg) concentration of CuATSM (Low) yielded a pure copper concentration of 0.18 g/kg within the hypoxic tumor region, this is taking into account the atomic composition (0.197) and uptake factor (9). It has been found that the lethal dose (LD50) for DMSO is 25 g/kg in subcutaneous injections in mice.⁴⁶ With the solubility of CuATSM in DMSO of 15 mg/mL and assuming a density of DMSO of 1.1 g/mL, the maximum concentration of CuATSM at this lethal dose would be 0.34 g/kg (Medium).⁴⁴ Additionally, initial CuATSM injections of the same concentration (1.35 g/kg) as the GNP model were used (High), as well as a very high concentration (Very-High) of 6.85 g/kg CuATSM (1.35 g/kg pure copper) to gain insight into how copper would act to enhance dose with the same injection concentration of gold. However, it should be noted that this is a theoretical target concentration, requiring a large volume of DMSO and would require another lower toxicity solvent to achieve this concentration (Table 1).

A hybrid scenario, using a combination of GNP (1.35 g/kg) in normoxic tissue, with CuATSM (2.6 g/kg) in hypoxic regions was also evaluated to generate a uniform dose enhancement across the total tumor (Mix).

Results

The radiosensitivity for copper and gold at various concentrations is quantified by calculating the percent depth dose along the central axis which is then normalized to dose in pure water for each beam source. Maximum DEF values are found at the front side of the slab with a decrease in dose deposition deeper within the slab (Figure 4A). The DEF is

below unity within the water phantom beyond the slab due to photon depletion. In all cases, the dose enhancement is greater in gold than in copper for equal concentrations.

To investigate the effects of beam hardening as a function of depth, the metal solution layer is moved within the phantom from 1 cm to 6 cm from the phantom surface (Figure 4B). The largest decrease in dose across the range for copper solutions is approximately 31%, for the SARRP beam. The dose decrease for the Carbon Target beam is 11% in the copper slab and the decrease was 0.5% for the Varian Trilogy model.

The concentration of metal within the inhomogeneity has a substantial effect on the maximum DEF (Figure 4C). At concentration of 0.1 g/kg, the DEF is below 1.02 in all cases.

Dose enhancements in the hypoxic tumor model used the SARRP beam for all simulations. Nearly all the CuATSM simulations show entry and exit DEFs close to unity within the normoxic tumor region, with the exception of the Very High concentration case which has a DEF of about 1.04 in the normoxic regions. Within the hypoxic core region, the DEF increases linearly with concentration from about 1.007 in the Low concentration case to 1.34 in the Very High concentration case.

All GNP simulations exhibit a DEF of approximately 1.13 within the proximal normoxic tumor region and 1.12 distally (Figure 5). Within the hypoxic core region, the DEF decreases from normoxic levels for all GNP cases, and is near unity for the Zero concentration GNP case. The Reduced GNP model has a DEF within the hypoxic region of 1.04, slightly higher than the copper for diagnostic CuATSM concentrations.

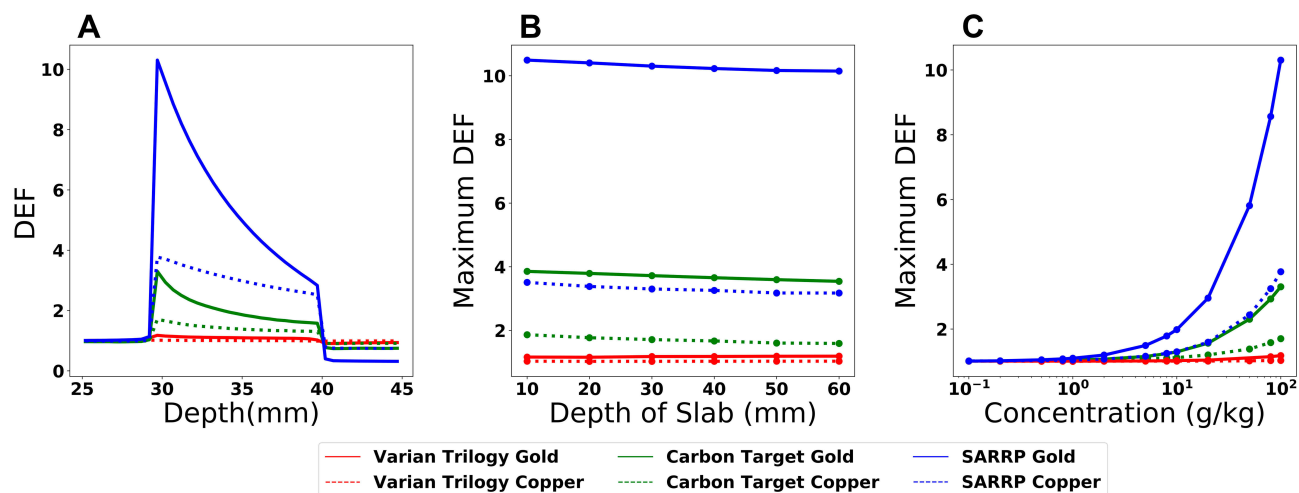


Figure 4 Parameters affecting the dose enhancement factor (DEF) within an inhomogeneous phantom for various beam qualities. **(A)** The DEF distribution within a 1 cm slab from 30 to 40 mm with a concentration of 100 g/kg **(B)** Depth of slab within phantom changed from 1 cm to 6 cm from front face. **(C)** Concentration of metal in inhomogeneity dependency on maximum DEF.

Abbreviations: SARRP, Small Animal Radiation Research Platform; DEF, dose enhancement factor.

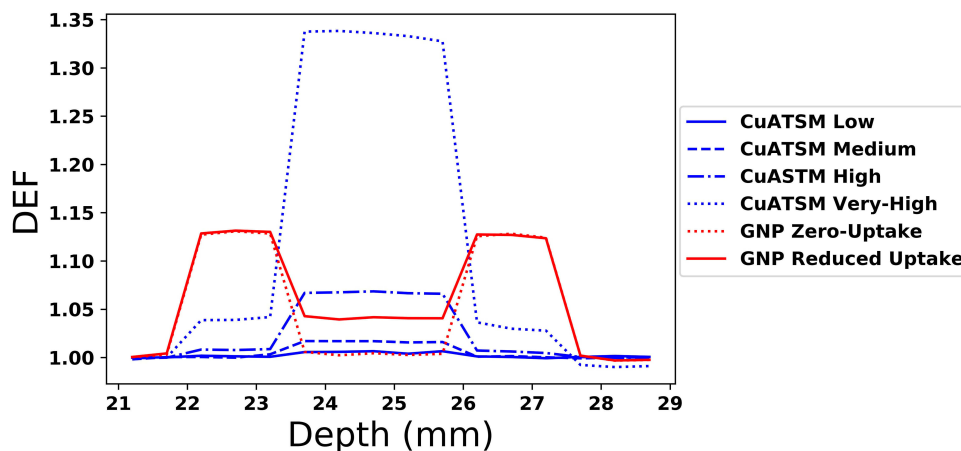


Figure 5 Hypoxic core tumor model; the DEF in cuboidal geometry with concentrations within hypoxic and normoxic regions as noted from literature.

Abbreviations: GNP, gold nanoparticle; CuATSM, Cu(II) diacetyl-bis N4-methylthiosemicarbazone; DEF, dose enhancement factor.

In the hybrid scenario, combining GNP and CuATSM, the resultant distribution across the entire tumor is more uniform (Figure 6).

Discussion

Dose escalation using metal radiosensitizers has been shown to result in the largest enhancement when treatment is combined with low energy photon beams, due to the increased probability for photoelectric interaction at low energy.^{48,49} To that end, models of the SARRP and a carbon target beam with the expectation that the dose escalation would be higher than for conventional treatment (6 MV) and still available for average clinics. As predicted, both the SARRP and carbon target beams had

higher DEF for the same concentration of metal radio-sensitizer compared to conventional 6 MV treatment.

Our results also suggest that lowering the energy of the photons would further increase the DEF due to the photoelectric effect. However, the practicality of using a low energy external beam is generally limited to shallow treatments; deeper treatment would require higher MV energies that would lower the photoelectric effect and lower the corresponding DEF from the mechanism explored here.^{13,15} The phantom models which varied the metal solution layer depth indicate that the decrease in dose enhancement due to the depth was moderate (31% over 5 cm depth) and, as expected, more pronounced for the lower energy spectra as beam hardening decreases the low energy photon fluence.

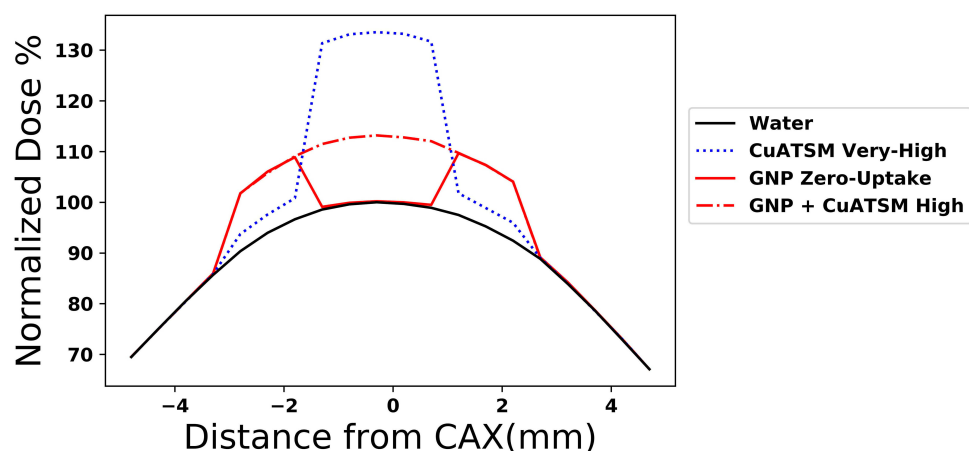


Figure 6 Dose profile of radiosensitizers normalized to maximum dose in water. The synthesis model with GNP and CuATSM has a uniform dose profile over the tumor area compared to the zero hypoxic uptake model. Very High concentration CuATSM shown for scale.

Abbreviations: GNP, gold nanoparticle; CuATSM, Cu(II) diacetyl-bis N4-methylthiosemicarbazone; CAX, central axis.

This would relate to a decreased DEF with either depth of the tumor or increase in tumor size where the shallow side would appreciate a greater DEF than the deeper lying side.

Concentration of metal deposited is one of the most important considerations in radiosensitizing. In practical applications, biological considerations of deposition and toxicity affect the maximum concentrations achievable in tumors. GNP have been investigated for potential toxicity and, with some exceptions, have been found to have low toxicity.^{43,50} Currently, the low solubility of CuATSM requires high levels of DMSO in order to reach concentrations comparable to GNP, and therefore high concentrations of CuATSM are limited due to the toxicity of DMSO. Although direct injection into a tumor could alleviate some effects from systemic injections, the feasibility of CuATSM as a radiosensitizer ultimately depends on future advancements in water soluble Bis(thiosemicarbazonato)copper(II) complexes that may eliminate the ceiling imposed by DMSO toxicity, or the replacement of DMSO with a non-toxic solvent.⁵¹ The highest concentration of copper considered (Figure 4) showcases the potential ability of CuATSM to radiosensitize hypoxic regions if DMSO toxicity is overcome. The toxicity of copper would then be limiting factor as indicated by systemic uptake in critical organs.^{42,52,53} Copper is a toxic heavy metal, which can result in organ damage upon accumulation. The authors suggest that an injection directly into superficial tumor tissue could reduce distal organ damage. Alternatively, researchers utilizing ⁶⁴CuATSM for radiotherapy have investigated the implementation of a copper chelating agent, penicillamine, to reduce copper doses to critical organs accumulators.⁵⁴

The intent of this research was to consider how hypoxic tissue uptake of metal in these forms could affect treatment utilizing radiosensitizers based on dose predictions from literature-based concentration levels. Tumors have complex geometries and oxygen distributions, however for simplicity, geometric approximations were introduced in the creation of the model. The tumor was approximated by three concentric cuboids, with normal tissue forming the exterior body. The tumor encompassed by the body was composed of tissue with normoxic and hypoxic regions. Additionally, the uptake values used for both GNP and CuATSM were based on single experiments and may not hold generally to changes in GNP geometries and coatings or different cell lines. The major implications of this investigation are that while GNP provide a high DEF in normoxic tissues, it should be expected that their uptake and therefore dose enhancement will diminish in the hypoxic regions present in most solid tumors. In one scenario, decreased uptake in hypoxic regions is caused by diminishing metabolic energy available in hypoxic tissues by which to endocytose.¹⁹ A more extreme scenario would occur with significant distance from vasculature where the successive layers of cells act to shield the hypoxic regions from GNP uptake, and the uptake decreases concentrations below radiosensitizing levels. In either scenario, the model indicates a decreased dose enhancement in hypoxic regions compared to normoxic regions: from 10% to 3% in the Reduced case, for the concentrations used here. Such a decrease could lead to higher survivability in tumors planned to receive uniform radiosensitized dose, and indicates that hypoxic regions

should have GNP uptake verified through imaging and mapped against hypoxia to ensure consistent radiosensitization. Conveniently, radiolabeled CuATSM has shown potential to act as a hypoxic map which may present a helpful utility for future CuATSM radiosensitization research.²⁶ A hypoxic tumor-targeting radiosensitizer would improve dose delivery to the most resistant part of the tumor as well as reduce patient alignment errors to target tumors with external beam radiation.

Conclusion

Hypoxic radioresistance has in many ways been the primary motivator of radiosensitizer development. GNP have potential to act as radiosensitizers in tumors, but are limited in their ability to radiosensitize hypoxic tumors uniformly. CuATSM is used in PET imaging of hypoxia, and does show some modest external beam radiosensitizing potential for hypoxic regions at diagnostic concentrations (≤ 0.1 g/kg). Direct injection to the tumor presents the most effective mechanism to achieve higher concentration, and therefore higher dose enhancements. A potential hybrid radiosensitization therapy utilizing GNP and CuATSM could map hypoxic regions and enhance dose uniformly across tumors allowing for decreased doses to non-target tissues and boosted doses in radioresistant hypoxic areas.

Acknowledgments

We thank Dr. Thilakshan Kanesalingam and the Research and Development team at Xstrahl for providing EGSncr models and schematics for the Small Animal Radiation Research Platform and Dr. Dave Parsons for models of the MV imaging carbon graphite target linear accelerator modification.

Disclosure

The authors report no conflicts of interest in this work.

References

- Lee CT, Boss MK, Dewhirst MW. Imaging tumor hypoxia to advance radiation oncology. *Antioxid Redox Signal*. 2014;21:313–337. doi:10.1089/ars.2013.5759
- Thomlinson RH, Gray LH. The histological structure of some human lung cancers and the possible implications for radiotherapy. *Br J Cancer*. 1955;9:539–549. doi:10.1038/bjc.1955.55
- Farrell N. Metal complexes as radiosensitizers. *Prog Clin Biol Med*. 1989;10:90–109.
- Harada H. How can we overcome tumor hypoxia in radiation therapy? *J Radiat Res*. 2011;52:545–556. doi:10.1269/jrr.11056
- Barker HE, Paget JT, Khan AA, Harrington KJ. The tumour micro-environment after radiotherapy: mechanisms of resistance and recurrence. *Nat Rev Cancer*. 2015;15:409–425. doi:10.1038/nrc3958
- Kobayashi K, Usami N, Porcel E, Lacombe S, Le Sech C. Enhancement of radiation effect by heavy elements. *Mutat Res*. 2010;704:123–132. doi:10.1016/j.mrrrev.2010.01.002
- Rosa S, Connolly C, Schettino G, Butterworth KT, Prise KM. Biological mechanisms of gold nanoparticle radiosensitization. *Cancer Nanotechnol*. 2017;8:2. doi:10.1186/s12645-017-0026-0
- Asaithamby A, Chen DJ. Mechanism of cluster DNA damage repair in response to high-atomic number and energy particles radiation. *Mutat Res*. 2011;711:87–99. doi:10.1016/j.mrfimm.2010.11.002
- Zhang ZY, Van Steendam K, Maji S, et al. Tailoring cellular uptake of gold nanoparticles via the hydrophilic-to-hydrophobic ratio of their (co)polymer coating. *Adv Funct Mater*. 2015;25:3433–3439. doi:10.1002/adfm.201500904
- Jazayeri MH, Amani H, Pourfatollah AA, Pazoki-Toroudi H, Sedighimoghaddam B. Various methods of gold nanoparticles (GNPs) conjugation to antibodies. *Sens Biosensing Res*. 2016;9:17–22. doi:10.1016/j.sbsr.2016.04.002
- Bae YH, Park K. Targeted drug delivery to tumors: myths, reality and possibility. *J Control Release*. 2011;153:198–205. doi:10.1016/j.jconrel.2011.06.001
- Berbeco RI, Detappe A, Tsiamas P, Parsons D, Yewondwossen M, Robar J. Low Z target switching to increase tumor endothelial cell dose enhancement during gold nanoparticle-aided radiation therapy. *Med Phys*. 2016;43(1):436–442. doi:10.1118/1.4938410
- Jain S, Coulter JA, Hounsell AR, et al. Cell-specific radiosensitization by gold nanoparticles at megavoltage radiation energies. *Int J Radiat Oncol Biol Phys*. 2011;79:531–539. doi:10.1016/j.ijrobp.2010.08.044
- Kodiha M, Wang YM, Hutter E, Maysinger D, Stochaj U. Off to the organelles—killing cancer cells with targeted gold nanoparticles. *Theranostics*. 2015;5:357–370. doi:10.7150/thno.10657
- Rahman WN, Bishara N, Ackerly T, et al. Enhancement of radiation effects by gold nanoparticles for superficial radiation therapy. *Nanomedicine*. 2009;5(2):136–142. doi:10.1016/j.nano.2009.01.014
- Maeda H, Ueda M, Morinaga T, Matsumoto T. Conjugation of poly(styrene-co-maleic acid) derivatives to the antitumor protein-neocarzinostatin: pronounced improvements in pharmacological properties. *J Med Chem*. 1985;28:455–461. doi:10.1021/jm00382a012
- Yohan D, Cruje C, Lu XF, Chithrani DB. Size-dependent gold nanoparticle interaction at nano-micro interface using both monolayer and multilayer (tissue-like) cell models. *Nano-Micro Lett*. 2016;8(1):44–53. doi:10.1007/s40820-015-0060-6
- Dewhirst MW, Secomb TW. Transport of drugs from blood vessels to tumour tissue. *Nat Rev Cancer*. 2017;17:738–750. doi:10.1038/nrc.2017.93
- Jain S, Coulter JA, Butterworth KT, et al. Gold nanoparticle cellular uptake, toxicity and radiosensitisation in hypoxic conditions. *Radiother Oncol*. 2014;110:342–347. doi:10.1016/j.radonc.2013.12.013
- Neshatian M, Chung S, Yohan D, Yang C, Chithrani DB. Uptake of gold nanoparticles in breathless (hypoxic) cancer cells. *J Biomed Nanotechnol*. 2015;11(7):1162–1172. doi:10.1166/jbn.2015.2067
- Obata A, Yoshimi E, Waki A, et al. Retention mechanism of hypoxia selective nuclear imaging/radiotherapeutic agent Cu-diacetyl-bis(N4-methylthiosemicarbazone) (Cu-ATSM) in tumor cells. *Ann Nucl Med*. 2001;15:499–504. doi:10.1007/BF02988502
- Lewis J, Laforest R, Buettner T, et al. Copper-64-diacetyl-bis(N4-methylthiosemicarbazone): an agent for radiotherapy. *Proc Natl Acad Sci*. 2001;98(3):1206–1211. doi:10.1073/pnas.98.3.1206
- Lapi SE, Lewis JS, Dehdashti F. Evaluation of hypoxia with copper-labeled diacetyl-bis(N-methylthiosemicarbazone). *Semin Nucl Med*. 2015;45(2):177–185. doi:10.1053/j.semnuclmed.2014.10.003
- Colombie M, Gouard S, Frindel M, et al. Focus on the controversial aspects of (64)Cu-ATSM in tumoral hypoxia mapping by PET imaging. *Front Med*. 2015;2:58. doi:10.3389/fmed.2015.00058

25. Dearling JJJ, Packard AB. Some thoughts on the mechanism of cellular trapping of Cu(II)-ATSM. *Nucl Med Biol.* 2010;37:237–243. doi:10.1016/j.nucmedbio.2009.11.004
26. Chao KS, Bosch WR, Mutic S, et al. A novel approach to overcome hypoxic tumor resistance: Cu-ATSM-guided intensity-modulated radiation therapy. *Int J Radiat Oncol Biol Phys.* 2001;49:1171–1182. doi:10.1016/S0360-3016(00)01433-4
27. Clausen MM, Hansen AE, Lundemann M, et al. Dose painting based on tumor uptake of Cu-ATSM and FDG: a comparative study. *Radiat Oncol.* 2014;9(1):228. doi:10.1186/s13014-014-0228-0
28. Obata A, Kasamatsu S, Lewis JS. Basic characterization of ⁶⁴Cu-ATSM as a radiotherapy agent. *Nucl Med Biol.* 2005;32:21–28. doi:10.1016/j.nucmedbio.2004.08.012
29. McMillan DD, Maeda J, Bell JJ, et al. Validation of ⁶⁴Cu-ATSM damaging DNA via high-LET Auger electron emission. *J Radiat Res.* 2015;56:784–791. doi:10.1093/jrr/rrv042
30. Laster BH, Shani G, Kahl SB, Warkentien L. The biological effects of Auger electrons compared to α -particles and Li ions. *Acta Oncol.* 1996;35:917–923. doi:10.3109/02841869609104046
31. Aghevlian S, Boyle AJ, Reilly RM. Radioimmunotherapy of cancer with high linear energy transfer (LET) radiation delivered by radionuclides emitting α -particles or Auger electrons. *Adv Drug Deliv Rev.* 2017;109:102–118. doi:10.1016/j.addr.2015.12.003
32. Yoshii Y, Furukawa T, Kiyono Y, et al. Internal radiotherapy with copper-64-diacetyl-bis (N4-methylthiosemicarbazone) reduces CD133+ highly tumorigenic cells and metastatic ability of mouse colon carcinoma. *Nucl Med Biol.* 2011;38:151–157. doi:10.1016/j.nucmedbio.2010.08.009
33. Kawrakow I, Rogers DWO. The EGSnrc code system. National Research Council Report No. PIRS-701. 2003.
34. Anderson J, Burns PJ, Milroy D, Ruprecht P, Hauser T, Siegel HJ. Deploying RMACC summit: an HPC resource for the rocky mountain region. *Proceedings of PEARC17.* New Orleans, LA; 2017. doi:10.1145/3093338.3093379. Available from: <https://www.colorado.edu/rc/resources/summit/citations>
35. Rogers DWO, Faddegon BA, Ding GX, Ma C-M, Wei J, Mackie TR. BEAM: a Monte Carlo code to simulate radiotherapy treatment units. *Med Phys.* 1995;22:503–524. doi:10.1118/1.597552
36. Parsons D, Robar JL, Sawkey D. A Monte Carlo investigation of low-Z target image quality generated in a linear accelerator using Varian's VirtuaLinac. *Med Phys.* 2014;41(2):021719. doi:10.1118/1.4861818
37. Tryggestad E, Armour M, Iordachita I, Verhaegen F, Wong JW. A comprehensive system for dosimetric commissioning and Monte Carlo validation for the small animal radiation research platform. *Phys Med Biol.* 2009;54:5341–5357. doi:10.1088/0031-9155/54/17/017
38. Malmir S, Mowlavi AA, Mohammadi S. Evaluation of dose enhancement in radiosensitizer aided tumor: a study on influential factors. *Rep Radiother Oncol.* 2015;2(4). doi:10.5812/rro.11076
39. Zabihezadeh M, Moshirian T, Ghorbani M, Knaup C, Behrooz MA. A Monte Carlo study on dose enhancement by homogenous and inhomogeneous distributions of gold nanoparticles in radiotherapy with low energy X-rays. *J Biomed Phys Eng.* 2018;8:13–28.
40. Ranjbar H, Shamsaei M, Ghasemi MR. Investigation of the dose enhancement factor of high intensity low mono-energetic X-ray radiation with labelled tissues by gold nanoparticles. *Nukleonika.* 2010;55(3):307–312.
41. Burgman P, O'Donoghue JA, Lewis JS, Welch MJ, Humm JL, Ling CC. Cell line-dependent differences in uptake and retention of the hypoxia-selective nuclear imaging agent Cu-ATSM. *Nucl Med Biol.* 2005;32:623–630. doi:10.1016/j.nucmedbio.2005.05.003
42. Yoshii Y, Furukawa T, Matsumoto H, et al. ⁶⁴Cu-ATSM therapy targets regions with activated DNA repair and enrichment of CD133+ cells in an HT-29 tumor model: sensitization with a nucleic acid antimetabolite. *Cancer Lett.* 2016;376:74–82. doi:10.1016/j.canlet.2016.03.020
43. Hainfeld JF, Slatkin DN, Smilowitz HM. The use of gold nanoparticles to enhance radiotherapy in mice. *Phys Med Biol.* 2004;49:N309–N315. doi:10.1088/0031-9155/49/18/N03
44. Williams JR, Trias E, Beilby PR, et al. Copper delivery to the CNS by CuATSM effectively treats motor neuron disease in SOD(G93A) mice co-expressing the Copper-Chaperone-for-SOD. *Neurobiol Dis.* 2016;89:1–9. doi:10.1016/j.nbd.2016.01.020
45. Noel PR, Barnett KC, Davies RE, et al. The toxicity of dimethyl sulphoxide (DMSO) for the dog, pig, rat and rabbit. *Toxicology.* 1975;3:143–169. doi:10.1016/0300-483X(75)90081-5
46. Willhite CC, Katz PI. Toxicology update: dimethyl sulfoxide. *J Appl Toxicol.* 1984;4:155–160. doi:10.1002/jat.2550040308
47. WebQC Chemical Portal. Molar mass calculator. Available from: <https://www.webqc.org/mmolcalc.php>. Accessed April 27, 2018.
48. Paro AD, Hossain M, Webster TJ, Su M. Monte Carlo and analytic simulations in nanoparticle-enhanced radiation therapy. *Int J Nanomedicine.* 2016;11:4735–4741. doi:10.2147/IJN.S114025
49. Jain S, Hirst DG, O'Sullivan JM. Gold nanoparticles as novel agents for cancer therapy. *Br J Radiol.* 2012;85:101–113. doi:10.1259/bjr/59448833
50. Alkilany AM, Murphy CJ. Toxicity and cellular uptake of gold nanoparticles: what we have learned so far? *J Nanopart Res.* 2010;12:2313–2333. doi:10.1007/s11051-010-9911-8
51. Buncic G, Hickey JL, Schieber C, et al. Water-soluble Bis(thiosemicarbazonato)copper(II) Complexes Aust. *J Chem.* 2011;64:244–252.
52. US Department of Health and Human Services. Toxicological Profile for Copper – U.S. Public health service agency for toxic substances and disease registry. 2004.
53. Stern BR. Essentiality and toxicity in copper health risk assessment: overview, update and regulatory considerations. *Toxicol Environ Health.* 2010;73:114–127. doi:10.1080/15287390903337100
54. Yoshii Y, Matsumoto H, Yoshimoto M, et al. Controlled administration of penicillamine reduces radiation exposure in critical organs during ⁶⁴Cu-ATSM internal radiotherapy: a novel strategy for liver protection. *PLoS One.* 2014;9(1):e86996. doi:10.1371/journal.pone.0086996

International Journal of Nanomedicine

Publish your work in this journal

The International Journal of Nanomedicine is an international, peer-reviewed journal focusing on the application of nanotechnology in diagnostics, therapeutics, and drug delivery systems throughout the biomedical field. This journal is indexed on PubMed Central, MedLine, CAS, SciSearch®, Current Contents®/Clinical Medicine,

Submit your manuscript here: <https://www.dovepress.com/international-journal-of-nanomedicine-journal>

Dovepress

Journal Citation Reports/Science Edition, EMBASE, Scopus and the Elsevier Bibliographic databases. The manuscript management system is completely online and includes a very quick and fair peer-review system, which is all easy to use. Visit <http://www.dovepress.com/testimonials.php> to read real quotes from published authors.